Experimental and FEM Analysis of the Bending Behaviour of Superelastic Tubing

Pelton, Rebelo, Duerig, Wick

The 1st Int'l Conference on Shape Memory and Superelastic Technologies 1994
(eds.) A. Pelton et al.
pp. 353-358

1994

Proceedings of the First International Conference on Shape Memory and Superelastic Technologies
Asilomar Conference Center, Pacific Grove, California, USA, 1994

EXPERIMENTAL AND FEM ANALYSIS OF THE BENDING BEHAVIOR OF SUPERELASTIC TUBING

A.R. Pelton*, N. Rebelo, T.W. Duerig* and A. Wick*****

* Nitinol Devices & Components, Inc. (NDC) 48501 Warm Springs Blvd., Suite 117, Fremont, California 94539, USA
** Hibbitt, Karlsson and Sorenson (West), Inc., 3900 Newpark Mall Road, Suite 302, Newark, California 94560, USA
*** NDC and Universität Karlsruhe, Institute für Werkstoffkunde I, 76128 Karlsruhe, GERMANY

ABSTRACT

The mechanical properties of superelastic Ni-Ti wires and microtubes were characterized to determine the criteria for buckling. Microtubes with OD/ID ratios from 1.09 to 1.80 were tested in uniaxial tension and three-point bending mode to large deflections. Since existing elasticity theories are inadequate to model bending and buckling of superelastic Ni-Ti, a finite element analysis model was developed. The calculated results are in close agreement with the experimental data. The implications of this study are discussed in terms of designing with superelastic microtubing.

INTRODUCTION

Superelastic NiTi alloys are increasingly being used in medical applications because of their ability to survive large deflections at a constant stress without permanent plastic strain. Wire is the predominant form of superelastic Nitinol, and is used for applications such as guidewires and orthodondic arches. Medical design engineers are also interested in other forms of the material, especially microtubing for use in components for endoscopic instruments, stents, and catheters. For these designers, it is critically important to characterize the bending behavior of the tubes as well as to predict the criteria for buckling.

The mechanical properties of superelastic wire have been studied in great detail; traditional uniaxial tensile stress-strain curves have been well documented. However, there has been a long-time quest to derive the constitutive relationships that govern the mechanical behavior of Ni-Ti under different modes of deformation. For example, Melton [1] noted the differences in the stress-strain curves of martensitic Ni-Ti-Cu under tensile, compressive and torsional deformation. He showed that at equivalent strain, stress was lowest in torsion, highest in compression, with intermediate values for tension. More recently, Adler, et al. [2] studied the mechanical behavior of binary Ni-Ti in tension, torsion and compression (unpublished) from -180 to 200°C. They showed that the superelastic behavior was similar in tension and torsion. Several other authors at this conference have also recognized the need to characterize superelastic Ni-Ti in other deformation modes, such as 3-point, 4-point and pure bending to better simulate actual application environments [3,4]. There is, however, a lack of consensus on how to interpret and to analyze the resulting mechanical data.

Furthermore, there is a dearth of experimental and analytical data on superelastic microtubes. Therefore, the focus of this article is to compare bending moment-curvature data from wire and microtubes with a finite element model, which is based on fundamental properties. Three-point bending was selected as the primary mode of deformation in order to present a worst-case scenario for tube buckling.

EXPERIMENTAL PROCEDURE

Superelastic Ni-Ti wires and microtubes were tested in tension, compression and bending with an Instron mechanical testing machine with tension-compression 5000lb and 1000g load cells. Sample deflections were measured in tension with an extensometer, and in compression and bending with an LVDT. Bending data were obtained with both 3-point and 4-point loading, although only 3-point bending results are reported here. The bending apparatus had a variable span from <10mm to >30mm to accommodate various sample diameters to achieve required strains.

RESULTS AND DISCUSSION

A typical load-deflection curve from a 1.5mm diameter wire with a 20mm span is shown in Fig. 1. Note that the curve exhibits the key attributes of superelasticity for medical applications, with well-defined upper and lower plateaus with essentially zero permanent set. According to elasticity theories [5], load can be converted into stress as **MY/I**, where **Y** is the distance from the neutral axis; **Y** equals the wire radius, **R**. **M**, the bending moment, is **Wl/4**, where **W** is the applied load and **l** is the span length. **I**, which is the second moment of inertia for the wire, is $\pi R^4/4$. Strain is calculated as $R\kappa$, where κ is the curvature of the neutral axis.

The above traditional equations are applied to the load-deflection data from Fig. 1 and compared to a stress-strain curve from a tensile test on the same wire as shown in Fig. 2. There are major differences between these two curves. The upper plateau stress for the wire deformed in uniaxial tension is approximately 550 MPa, which is typical for optimized superelastic wire. In bending, the apparent plateau stress (measured at 4% strain) is nearly 1200 MPa, which is obviously too high. Berg [6] also observed such discrepancies in the stress - strain curves between bending and tension modes of deformation. Therefore, he was unable to model the bending behavior of Nitinol wires from the tensile properties. Berg assumed that the tension and compression modes of deformation were identical, which is contrary to published data for bulk samples [1,2,7]. In order to obtain more realistic results for the present investigation, the tensile and compression data from 1.8mm diameter Nitinol wire are compared in Fig. 3. This figure demonstrates the differences in the properties of Nitinol wire in tension and compression. Since traditional "strength of materials" approaches to mechanical behavior are governed by tension - compression equivalence, it is clear that these methods are inappropriate for superelastic material. Therefore, a finite element model was developed to understand the experimental data more fully; this model is described in the following section.

Finite Element Analysis

These calculations are a simple attempt at applying currently available commercial stress analysis codes to the simulation of deformation of tubing. The general purpose finite element program ABAQUS [8] was used in this instance. The material model used corresponds to a nonlinear elastic material, although it is recognized that this is a very crude approximation to the true behavior of superelastic Nitinol. Hyperelasticity theory was used, in which the strain energy function is represented via the Ogden formulation. In such case, the strain energy function (energy per unit original volume) is as follows:

$$U = \sum_{i=1}^{N} \frac{2\mu_i}{\alpha_i^2}\left(\overline{\lambda}_1^{\alpha_i} + \overline{\lambda}_2^{\alpha_i} + \overline{\lambda}_3^{\alpha_i} - 3\right) + \sum_{i=1}^{N} \frac{1}{D_i}(J-1)^{2i}$$

where N is the order of the polynomial; μ_i, α_i, D_i are material constants

$\overline{\lambda}_j = J^{-\frac{1}{3}}\lambda_j$ with λ_j principal stretches

J is the Jacobian of the deformation gradient ; J - 1 is the volumetric strain

The first terms of the function represent deviatoric behavior, and the last terms represent the volumetric behavior. It was felt that we could model the material as incompressible, since the deformation we are trying to model is predominantly uniaxial; errors in the volumetric representation would translate mainly into small changes in crossection dimensions. Therefore, volumetric strain energy terms are neglected. Special elements which impose an incompressibility constant via Lagrangean multipliers were used throughout.

The material constants are by no means obvious, nor do they have physical meaning. ABAQUS will internally determine these constants by doing a least squares fit of the strain energy function with respect to experimental results. A uniaxial curve made out of pairs of nominal stress versus nominal strain values were provided to the code, and a best fit is obtained for a given polynomial order. This procedure allows for substantially different behavior in tension and in compression, provided that the uniaxial curve supplied has the results of both compression and tension tests. Fig. 3 represent the experimental curves supplied and a simulated reproduction of the uniaxial test. Note in this figure that the model simulates the tension data quite well, and the fit to the compression data has slightly greater deviations. Nevertheless, we feel that this material representation is quite adequate for the bending simulations we have carried out.

Bending, to the levels we have tested, translates mainly in local uniaxial behavior, which we seem to reproduce well. However, severe limitations of this mathematical model should be pointed out, and attempts at simulating other types of behavior should be carried out with extreme caution. First, if we were to unload the model, the behavior would follow exactly the loading path in reverse. This is a pure elastic model, without hysteresis effects. Second, if behavior other than uniaxial is to be modeled, then more test data would be required. It is well known that these models do not extrapolate well from tests of one type of behavior to analysis of another type of behavior. Nor can these analyses be extrapolated beyond the strain range of the tests provided, especially for higher order polynomials.

In the context of this study, the limitations of the model discussed above are minor. We are mainly interested here in the stress- and strain-distributions of wire and microtubes and in loading and

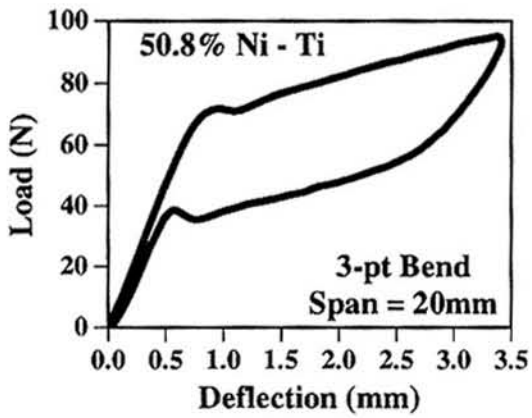

Figure 1: Load-Deflection curve of 1.5mm wire in 3-point bending.

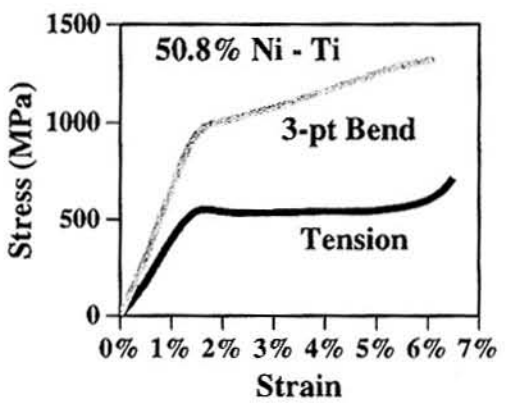

Figure 2: Comparison of stress-strain curves from 3-point bending and tension.

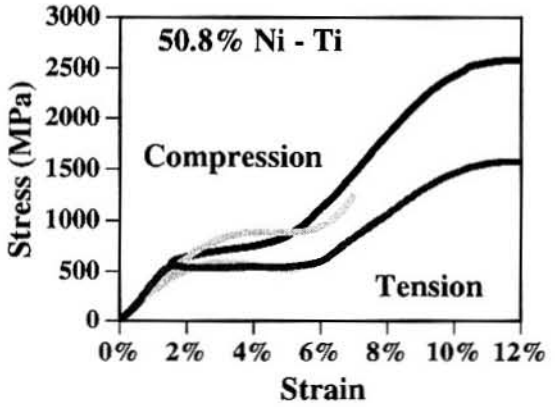

Figure 3: Stress-strain comparison of tension and compression deformation of wire. Superimposed are data from FEA model.

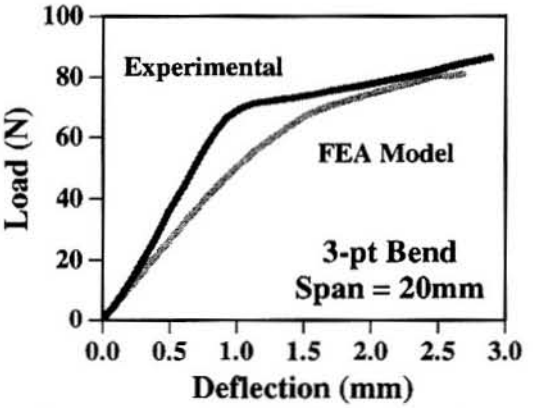

Figure 4: Comparison of experimental and FEA model in 3-point bending.

buckling behavior of microtubes. Fig. 4 shows the results of the model compared with the initial load - deflection data from the 1.5mm superelastic wire (Fig. 1). The bending modulus predicted by the model is slightly lower than the experimental data. At larger deflections, however, the model fits the experimental data extremely well. It should be also pointed out that the experimental tensile and compressive data were also fit to elastic-plastic models with substantially worse coefficient of fit.

Fig. 5 illustrates the strain distribution in a 1.5mm diameter wire at 2.7mm deflection in 3-point bending. It is immediately obvious from this figure that the neutral axis has moved toward the compression surface with respect to the initial position and that the maximum tensile strain in the outer fiber is approximately 8%. From Fig. 2, however, the strength of materials calculations predicts only 5.5% strain at this deformation. It is also apparent that there is strain localization due to the nature of the non-uniform loading.

Similar testing was done on a family of superelastic Nitinol microtubing; Fig. 6 shows a load-deflection curve of a tube with OD/ID ratio of 1.42 (OD = 0.90mm, wall thickness = 0.13mm) with a 20mm span and maximum deflection of 3mm. The curve may be compared with Fig. 1, and demonstrates the expected characteristics of an optimized superelastic material. The loading portion from a series of load-deflection curves from tubes with different OD/ID ratios and with constant ID (0.635mm) are compared in Fig. 7. As expected, the thickest wall tubing has the highest apparent loading plateau and modulus.

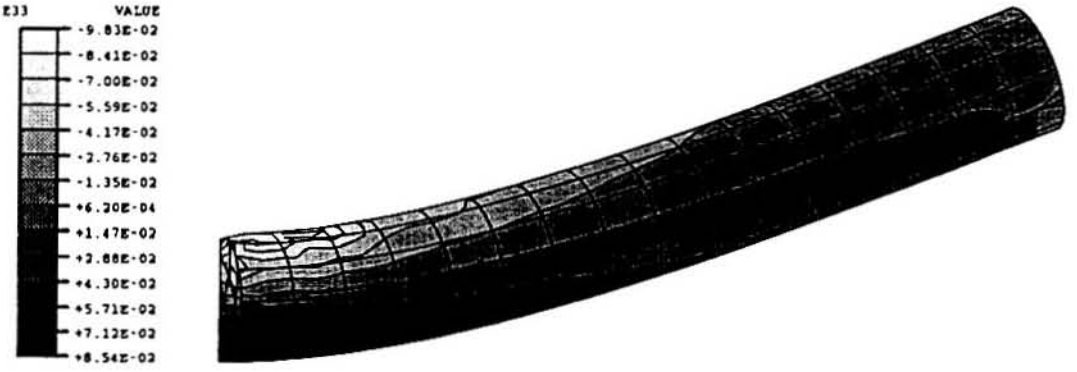

Figure 5: FEA model of 1.5mm diameter wire at 2.7mm deflection under 3-point bending.

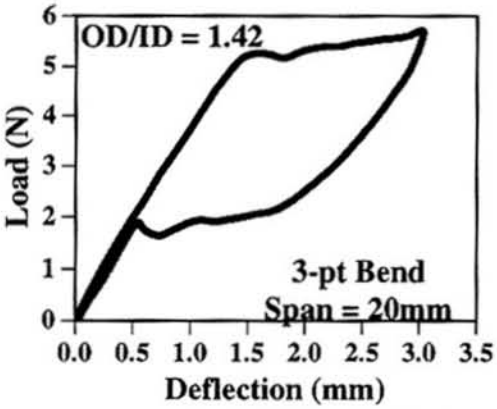

Fig. 6: Load-deflection curve of Nitinol microtubing with ID = 0.635m

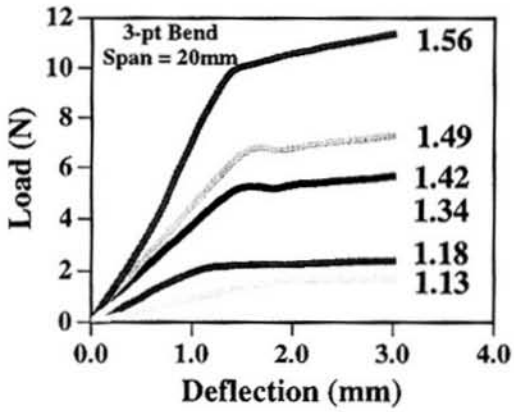

Fig. 7: Family of load-deflection curves microtubing with ID = 0.635mm

The thinner wall tubes (OD/ID = 1.18, 1.13) from this series were also tested with 10mm span in order to increase the strain for equivalent deflections. Fig. 8 shows the load-deflection curve of the 1.18 tube (OD = 0.75mm, wall thickness = 0.11mm). In contrast to the results shown in Fig. 7, the loading curve shows a small portion of constant plateau up to approximately 1.75mm deflection. There is a slight increase in the load up to a maximum at 2.5mm deflection and then a decrease to the unloading deflection of approximately 3.3mm. Note also that there is a large permanent set upon unloading to zero load. Visual inspection of the tube during the tests showed that the tube began to become oval between 1.0 and 1.5mm deflection, with buckling at about 2.5 - 2.75mm. Tubes that were unloaded after 1.5mm deflection fully returned to circular crossection with no permanent set.

FEA was used to characterize this macroscopic bending and buckling behavior of the above tubes. As with the wire, tubes were tested in tension to provide the model with a framework for analysis. However, due to the difficulties with testing microtubing in compression, data from the wires were used in the FEA model; there was a similar quality of fit. According to the model for the results shown in Fig. 8, tube ovalization began locally at about 1.0mm deflection, with corresponding maximum outer-fiber strains of approximately 3-4%. After 2.0mm deflection, the tube is severely oval with outer fiber strains of over 8% in compression and nearly 8% in tension, as illustrated in Fig. 9. In contrast, elasticity calculations predict less than 6% strain at 2mm deflection. The model demonstrates that there is a large strain gradient across the wall thickness, from high compression on the loading surface to high tension on the inner surface. It is also apparent that the neutral axis has moved toward the loading surface. Furthermore, the high strain gradients are very localized with maximum extent of about 1.25mm along the tube axis from the point of loading.

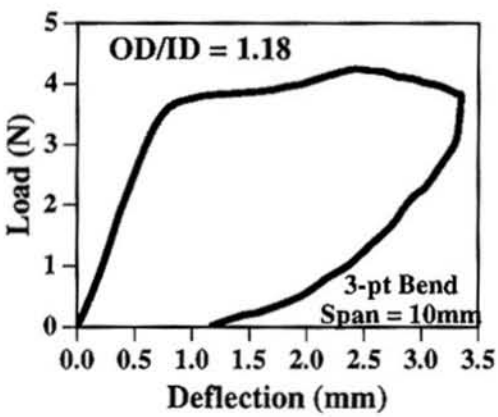

Figure 8: Load-deflection curve of tubing with ID = 0.635mm and span = 10mm.

A possible explanation for the macroscopic load-deflection behavior and microscopic strain distribution from FEA modeling can now be considered. As mentioned above, 3-point bending provides a worst case mode of deformation for tubing because of local stress concentrations. Thin-wall tubes begin buckling initially by tube ovalization, although this change in cross section geometry was not apparent on the macroscopic load-deflection curves. At higher deflections, there are regions of extreme strain concentration, that can exceed the limit of

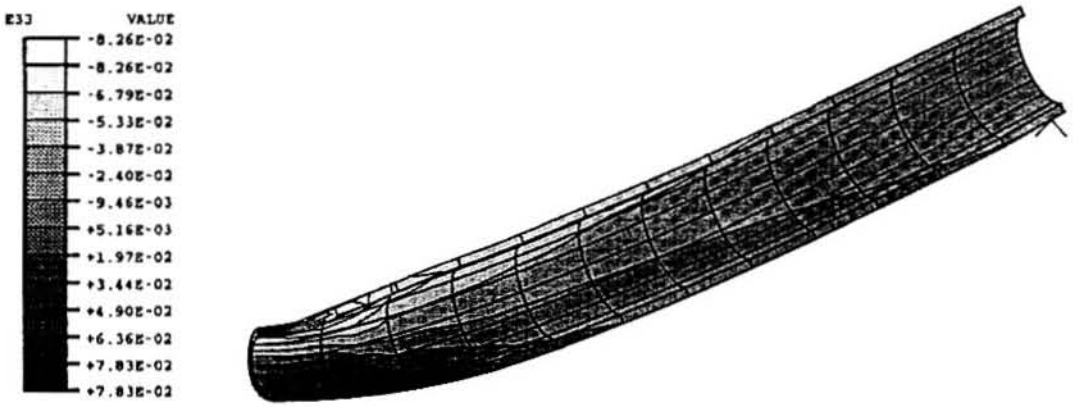

Fig. 9: FEA model of microtubing at 2.0mm deflection under 3-point bending; see Fig. 8.

superelasticity (i.e., greater than about 8%). As the local strain increases, strain hardening can occur in the affected region. When sufficient volume of the material has been over strained, there will be a higher resistance to loading, which can lead to an apparent ultimate tensile load and impending failure. In Fig. 8, the apparent UTS occurs at approximately 2.5mm deflection, which is followed by a load drop. This scenario was tested with several thin-wall tubes (OD/ID = 1.26, 1.18, 1.13, and 1.09) by strain cycling to increasingly higher deflections and then unloading and inspecting at 10x magnification. As long as the deflection was below the strain-hardening range, there was no permanent set upon unloading and the tube returned to a circular crossection. This is also in agreement with the FEA model that shows that at 2.0mm deflection, regions of the tube are near the superelastic limit of 8% strain.

Collectively, these results suggest that thin-wall Ni-Ti tubes can be used in bending as long as care is taken to prevent point loading. Preliminary results from "pure" and four-point bending tests indicate that buckling is less likely due to more uniform strain distributions. Therefore, with proper design, superelastic tubes can be employed in environments required for medical devices.

CONCLUSIONS

The mechanical properties of superelastic Ni-Ti wire and microtubes were studied systematically to understand their bending behavior. Conventional "strength of materials" formulations were inadequate to model the stress and strain response of wire in bending. Therefore, a model was developed with finite element analysis that incorporates both uniaxial tension and compression data. The model fits the experimental bending data within 10% rms. FEA was then used to characterize the bending and buckling behavior of microtubes. The model accurately predicts the localization of strain in thin-wall tubes in 3-point bending. Based on these results, correlations were made between the macroscopic load-deflection curves and microscopic strain distributions in microtubes.

REFERENCES

[1] K.N. Melton, Engineering Aspects of Shape Memory Alloys, eds. T.W. Duerig , et al., Butterworth-Heinemann, London, 21 (1990).
[2] P. Adler, et al. Scripta Met. **24**, 943 (1990).
[3] Y. Gillett, et al., Proc. ICOMAT, 1241 (1993); SMST Proceedings (1994).
[4] R. Zadno and P. Poncet, SMST Proceedings (1994).
[5] S. Timoshenko, et al., Elements of Strength of Materials, Van Nostrand Co., NY (1968).
[6] B.T. Berg, Army High Performance, pre-print 9163 (1991); submitted to JAM (1994).
[7] D.N. Petrakis, Proc. ICOMAT, 1283 (1993); SMST Proceedings.
[8] ABAQUS User's Manual, ver 5.3, Hibbitt, Karlsson & Sorensen, Inc., Pawtucket, RI 1993.